Trapping Cold Ground State Argon Atoms

P. D. Edmunds and P. F. Barker
Department of Physics and Astronomy, University College London, Gower Street, London WC1E 6BT, United Kingdom
(Received 12 June 2014; published 30 October 2014)

We trap cold, ground state argon atoms in a deep optical dipole trap produced by a buildup cavity. The atoms, which are a general source for the sympathetic cooling of molecules, are loaded in the trap by quenching them from a cloud of laser-cooled metastable argon atoms. Although the ground state atoms cannot be directly probed, we detect them by observing the collisional loss of cotrapped metastable argon atoms and determine an elastic cross section. Using a type of parametric loss spectroscopy we also determine the polarizability of the metastable $4s[3/2]_2$ state to be $(7.3 \pm 1.1) \times 10^{-39}$ C m^2/V. Finally, Penning and associative losses of metastable atoms in the absence of light assisted collisions, are determined to be $(3.3 \pm 0.8) \times 10^{-10}$ cm^3 s^{-1}.

DOI: 10.1103/PhysRevLett.113.183001 PACS numbers: 37.10.De, 34.50.Cx, 37.10.Gh

The development of methods to create, control, and manipulate the motion of cold atoms and molecules has, over the last ten years, allowed the study of atomic and molecular interactions with unprecedented precision. Cold molecules offer a new test bed for precision measurement [1], the exploration of cold collisions and chemistry [2], and for studying condensed matter physics [3] and even quantum information science [4]. Of central importance to these applications has been the development of dissipative cooling techniques to create translationally cold molecules that are in their absolute internal ground state.

Sympathetic cooling molecules using laser cooled atoms is a promising general method for dissipative cooling, but typical laser cooled species are reactive and cannot generally be utilized [5]. Trapped noble gas atoms in their ground state appear to be ideal candidates for the sympathetic cooling of molecules [6–8] as they are chemically inert and can be laser cooled to μK temperatures in an excited metastable state. Cold helium gas has been used to buffer gas cool many species, but temperatures are limited to the 100 mK range [9]. As these atoms are in their absolute ground state, inelastic state changing collisions which can prevent efficient collisional cooling can be reduced or avoided.

All noble gas atoms have been laser cooled in a metastable state [10–17] and all but helium can be quenched to its ground state by dipole allowed transitions. However, once in their ground state they have no magnetic moment and cannot be trapped in a magnetic trap. Ground state noble gas atoms can, however, be trapped using large optical fields detuned far from resonance even though their static polarizabilities are at least an order of magnitude smaller than typical laser cooled species [18–21]. Ground state noble gases are, however, difficult to detect spectroscopically since the first dipole allowed transitions are in the vacuum ultraviolet. They can however, in principle, be detected when simultaneously trapped with another species that can be probed spectroscopically. This can be accomplished because the interactions between the two species in a trap perturb the motion of the observable species via intratrap collisions. Examples include atomic ions that are sympathetically cooled by other trapped ions in the trap [22]. Detection is accomplished by modulating the trap potential to parametrically heat species that cannot be directly observed. This frequency is usually unique to each species because of their differences in mass. The modulation heats the species, which can be detected as a change in the fluorescence monitored from the trap. By recording the trap fluorescence as a function of modulation frequency a type of species-specific mass spectrometry has been achieved in ion traps. In neutral atom traps parametric heating is a well established way of characterizing the trap. For example, the loss induced by parametric heating is commonly used to identify trap frequency and therefore trap depth for a particular species [23]. In addition, by tuning slightly away from the parametric resonance, selective removal of hot atoms in the trap has been demonstrated [24].

In this Letter we describe dipole trapping of cold ground state argon atoms and their detection by using a type of parametric loss spectroscopy based on cotrapping a small fraction of metastable argon atoms. We measure the polarizability of the metastable state at the trapping wavelength of 1064 nm and the Penning and associative losses of trapped metastable atoms in the absence of resonant laser light. We determine the enhanced loss rate of metastable atoms by collisions with the cotrapped ground state atoms and derive elastic collision cross sections at room temperature and at ultracold temperatures.

The trapping and detection of ground state argon atoms in a dipole trap is shown schematically in Fig. 1. Metastable argon atoms are first Doppler cooled in a magneto-optical trap (MOT) on the $4s[3/2]_2$ to $4p[5/2]_3$ transitions [25] shown in Fig. 2. A fraction of these atoms are subsequently trapped in an optical lattice formed by an optical buildup cavity with a circulating power of $\sim$1 kW, which

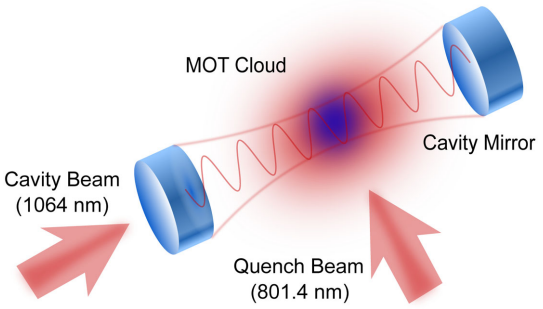

FIG. 1 (color online). Schematic of the optical cavity trap. Metastable argon is first cooled in a MOT, and then quenched down to the ground state. Both species can be trapped.

corresponds to a well depth of ~3 mK for metastable argon atoms and ~70 μK for ground state atoms [26]. The trapped metastable atoms are transferred to the ground state by optically quenching from the $4s[3/2]_2$ state using a laser at 801.4 nm. This laser first excites atoms from the $4s[3/2]_2$ to the $4p[5/2]_2$ state, from which they decay to the ground state via either the $4s[3/2]_1$ or $4s[1/2]_1$ states. By performing an incomplete quench we populate the trap with both ground state and metastable species.

The MOT is initially loaded for ~2 sec, after which the intracavity circulating power is ramped up over 30 ms to that required for trapping (1 kW) [26]. After this period the quench beam is switched on for 1–5 ms (depending on how many atoms we want to quench) and the Zeeman slower beam, MOT magnetic field, and MOT beams are all switched off and the atoms are held for the trapping period. To image atoms remaining after the trapping period, the MOT beams are switched back on and the remaining atoms are counted via their fluorescence recorded on a CCD camera.

As metastable argon atoms have intrinsically high internal energy, an intratrap collision can lead to either a Penning or associative ionization process where both metastable atoms are lost. For most metastable atoms, the non spin-polarized loss rate is of order 10^{-10} cm^3/s [10–17] and trap lifetimes are limited by these interactions.

Trap loss of metastable atoms in the optical lattice can be described by the differential equation,

$$\dot{\rho_e} = -\Gamma\rho_e(t) - \gamma_{ee}[\rho_e(t)]^2, \quad (1)$$

where ρ_e is the density of trapped metastable atoms, Γ is the one-body loss coefficient (i.e., mostly caused by collisions with background atoms) and γ_{ee} is the two-body loss coefficient (caused by metastable inelastic intratrap collisions). If the effective trap volume is not time dependent, the number of trapped atoms is given by

$$\rho_e(t) = \frac{\Gamma\rho_e(0)e^{-\Gamma t}}{\gamma_{ee}\rho_e(0)(1-e^{-\Gamma t}) + \Gamma}, \quad (2)$$

where $\rho_e(0)$ is the initial density of metastable atoms.

Figure 3 displays two lifetime curves; one loaded with only metastable atoms (black squares) and the other with both ground state and metastable atoms (red circles). Note

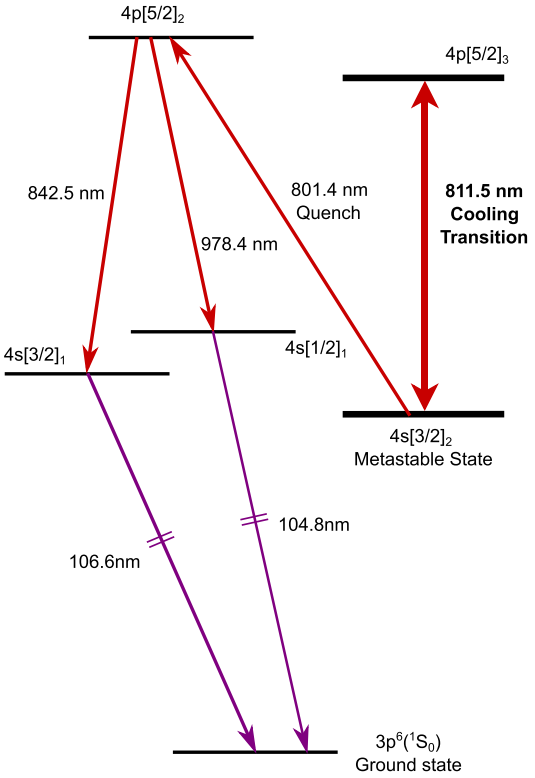

FIG. 2 (color online). Energy level diagram for argon, including relevant wavelengths for cooling and quenching to the ground state.

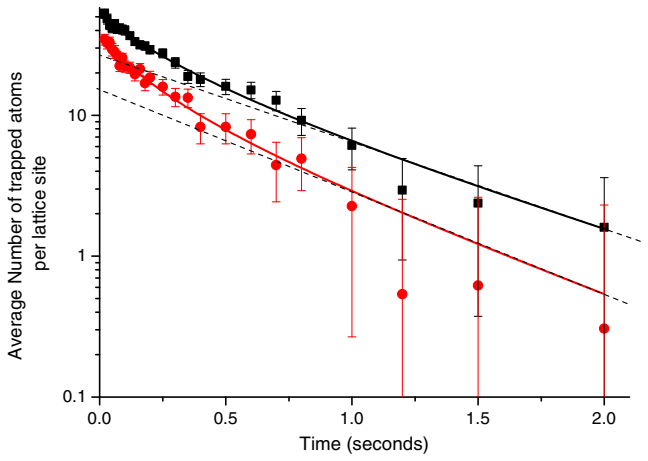

FIG. 3 (color online). Lifetime curves that plot the average number of trapped metastable atoms in a lattice trap as a function of time. Black squares correspond to only trapped metastable atoms. Red circles are for cotrapped metastable and ground state atoms. The dashed lines indicate the decay curve if only collisions with background gases caused trap loss. The error bars originate from the standard error of 20 images averaged for each data point.

that in each case the first few hundred milliseconds of the lifetime curve (highest density) deviates from a single exponential decay. We attribute this loss to Penning and associative losses for the case when only metastable atoms are loaded into the trap. The remaining loss after this time is primarily due to background collisions. To see this, an additional line has been placed on the graph demonstrating what the lifetime curve would be if only background collisions with a single exponential decay contributed. When both species are loaded into the trap the number of metastable atoms is observed to decrease more quickly when compared to the case of metastables only. This is discussed in detail further below.

Equation (2) was first fitted to the decay curve corresponding to only metastable atoms loaded into the trap. The one-body loss coefficient Γ was determined from the fit to be $1.3 \pm 0.1\ \mathrm{s}^{-1}$ and the two-body loss coefficient, γ_{ee}, is $(3.3 \pm 0.8) \times 10^{-10}\ \mathrm{cm}^3\ \mathrm{s}^{-1}$. Our two-body loss coefficient, γ_{ee}, is lower than a previously measured value [14] of $(5.8 \pm 1.7) \times 10^{-10}\ \mathrm{cm}^3\ \mathrm{s}^{-1}$. The previous value, however, is measured in a MOT without extrapolation to vanishing MOT light intensity. Light-assisted collisions artificially raise the measured value, which is in keeping with our lower value measured in the off-resonant lattice. The total cross section $\sigma_{ge} = \Gamma/\rho\bar{v}$ can be determined from the loss coefficient, where ρ is the background density of ground state argon in the vacuum chamber and $\bar{v}$ is the mean relative velocity. This gives a value of $(1.7 \pm 0.8) \times 10^{-13}\ \mathrm{cm}^2$ at room temperature. The error results primarily from uncertainty in the background pressure ($\sim 8 \times 10^{-9}$ mbar). This total cross section is a combination of elastic metastability exchange [27,28] and direct processes and corresponds well to a value of $5.6 \times 10^{-14}\ \mathrm{cm}^2$ determined at higher energy and with theoretical values [29,30].

Elastic collisions between metastable argon and ground state argon are known to dominate over inelastic processes [30–33]. While elastic collisions cannot lead to direct metastable loss when both metastable and ground state atoms are cotrapped, collisions will on average lead to loss of the ground state atoms. This is because the optical well depth for ground state atoms is approximately 40 times lower than for metastable atoms. This process leads to a type of sympathetic cooling of the metastable atoms which increases the metastable atom density leading to greater loss through Penning and associative inelastic collisions. This is what we observe in our experiments and is shown in Fig. 3. We model this loss process using Eq. (1), but now the trapped volume of the metastable atoms decreases with time. As we measure the metastable number as a function of time we obtain the volume or temperature dependence as a function of time as

$$V(t)(\propto T^{3/2}) = \frac{N(t)(\gamma_{ee}\frac{N_e(0)}{V(0)}(1-e^{-\Gamma t})+\Gamma)}{\Gamma\frac{N_e(0)}{V(0)}e^{-\Gamma t}}. \qquad (3)$$

From the data in Fig. 3 we obtain an e^{-1} thermalization time of 0.25 sec which can be equated to $\tau^{-1} = \sigma_{eg}(N_e + N_g/3V_{eg})\sqrt{(8k_B/\pi)((T_e+T_g)/m)}$ [34], where σ_{eg} is the total elastic cross section, N_e and N_g are the number of trapped metastable and ground state atoms per lattice sites, respectively, V_{eg} is the spatial overlap of the two atomic clouds, T_e and T_g are the metastable and ground state temperatures, and m is the atomic mass. We determine an approximate total elastic cross section of $\sim 6 \times 10^{-11}\ \mathrm{cm}^2$ using the measured initial temperatures, atom number, and thermalization time obtained from our data. This is larger than the total cross section at room temperature but is consistent with calculations of the elastic cross section of the nearby $(4s'[1/2]_0)$ metastable state as function of collision energy [30]. In Fig. 3 we show a decay curve where 35% of the metastable state is quenched. Larger ground state fractions produce a similar cross section but with a larger uncertainty due to a smaller signal-to-noise ratio.

To verify that we have trapped ground state atoms, we utilize a parametric heating technique. For a harmonic trap, the frequency of modulation at which significant heating and trap loss occurs is equal to $2\omega/n$, where ω is the trap frequency and n is an integer. The axial trap frequency in a harmonic trap is given by $\omega_z = 2\pi f_z = \sqrt{2(U_0 k^2/m)}$, where m is the mass of the trapped particle, U_0 is the well depth, and $k = 2\pi/\lambda$. U_0 is related to the polarizability by $U_0 = (2\alpha/\epsilon_0 c)I_c$, where I_c is the one-way circulating peak intensity. As the lattice wells are only harmonic for the lowest energy atoms the parametric heating spectrum is broadened [24,35]. In addition, as we load both ground and excited state atoms into the trap we expect to observe trap frequencies for both states. As we only observe the metastable state, the loss for the ground state has a different signature from that of loss from the metastable state. This is because if ground state atoms are ejected from the trap the lifetime of the metastable atoms in the trap is increased. Instead of a decrease in observed fluorescence when modulated on a parametric heating resonance, an increase is observed. When the trap frequency of the metastable atoms is reached, we observe the conventional decrease in fluorescence.

The trap frequencies for the metastable atoms were determined by applying a sinusoidal intensity modulation to the light coupled into the buildup cavity using an acousto-optic modulator. The well depth was modulated by 10% for frequencies up to 4 MHz for 100 ms. The trap was then turned off and the remaining metastable atoms were imaged on an EMCCD camera following illumination by the MOT beams. This provided a parametric loss spectrum as shown in Figs. 4(a) and 4(b).

Figure 4(a) shows two peaks corresponding to modulation at approximately the radial trap frequency and at twice this value, 1.7 and 3.0 kHz, respectively. Figure 4(b) shows

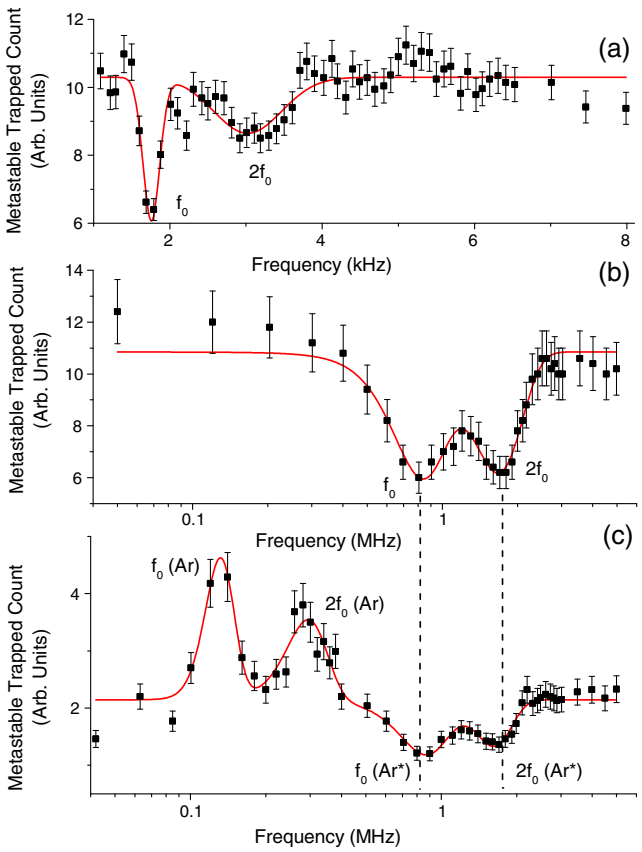

FIG. 4 (color online). Graph displaying parametric resonances of Ar and Ar* atoms observed in the dipole trap. (a) Two troughs due to metastable atoms being parametrically heated out of the trap at the radial trap frequencies. (b) The same as (a), but for the axial trap frequencies. (c) The axial trap frequencies when we cotrap ground state and metastable atoms together. The error bars are determined from fluctuations in 20 averaged fluorescence images.

two higher frequency peaks corresponding to modulation at the axial trap frequency and approximately twice this value along the lattice at 820 kHz and 1.67 MHz, respectively. These four frequencies correspond to an intracavity intensity of $\sim 7 \times 10^9$ W/m^2 using a polarizability of 5.51×10^{-39} C m^2/V [36]. To measure the ground state frequencies we quenched 80% of the metastables loaded into the trap. When the parametric loss measurements are repeated we observe four well-defined peaks as shown in 4(c). Two of these peaks, at frequencies of 130 and 300 kHz, correspond to the reduced loss of metastable atoms. These frequencies correspond to the trap frequency and twice its value. The other two peaks at 890 kHz and 1.75 MHz show increased loss due to direct conventional parametric excitation and are consistent with Fig. 4(b). We use these trap frequencies to determine the ratio of the polarizability of metastable to ground state argon, α_{ar*}/α_{ar}. Using both parametric resonances at f_z and $2f_z$ for both species, we calculate the α_{ar*}/α_{ar} ratio to be 40 ± 6. As the trap light is far from any resonance, the polarizability of the ground state should be well approximated by its static value given by 1.83×10^{-40} C m^2/V [37]. However, the metastable state polarizability is likely to be larger due to the trapping light at 1064 nm. We determine this polarizability by using the measured polarizability ratio and the assumption that the ground state value is well approximated by its static value. This gives a metastable polarizability of $(7.3 \pm 1.1) \times 10^{-39}$ C m^2/V, which as expected, is larger than the static polarizability of 5.51×10^{-39} C m^2/V.

We have trapped ground state argon atoms in an optical dipole trap for the first time and detected them using a parametric heating process. Detection of the ground state atoms was observed by a reduced loss of cotrapped metastable argon allowing the measurement of the polarizability of the metastable state and a total metastable-ground state elastic cross section at submillikelvin temperatures. By trapping only metastable argon we determined the one-body and two-body loss coefficients in the absence of light assisted collisions. The parametric heating method described here will allow the detection of other cotrapped dark species such as molecules which often have transitions where cw laser sources are not readily available. As the polarizability of most molecules is much larger than ground state argon the sympathetic cooling process we observe could also be utilized for molecules. Molecules could be loaded into the trap using methods such as Stark deceleration [6] before the argon atoms are loaded and quenched to their ground state. As the ground state is not limited by Penning losses, continual quenching may allow accumulation of ground state atoms above the 10^{10} cm^{-3} limit which is important for sympathetic cooling.

[1] H. Loh, K. C. Cossel, M. Grau, K.-K. Ni, E. R. Meyer, J. L. Bohn, J. Ye, and E. A. Cornell, Science **342**, 1220 (2013).
[2] A. Henson, S. Gersten, Y. Shagam, J. Narevicius, and E. Narevicius, Science **338**, 234 (2012).
[3] A. Micheli, G. Brennen, and P. Zoller, Nat. Phys. **2**, 341 (2006).
[4] A. André, D. DeMille, J. M. Doyle, M. D. Lukin, S. E. Maxwell, P. Rabl, R. J. Schoelkopf, and P. Zoller, Nat. Phys. **2**, 636 (2006).
[5] M. Lara, J. L. Bohn, D. Potter, P. Soldán, and J. M. Hutson, Phys. Rev. Lett., **97**, 183201 (2006).
[6] P. Barker, S. Purcell, P. Douglas, P. Barletta, N. Coppendale, C. Maher-McWilliams, and J. Tennyson, Faraday Discuss. **142**, 175 (2009).
[7] P. Barletta, J. Tennyson, and P. Barker, New J. Phys. **11**, 055029 (2009).
[8] J. M. McNamara, T. Jeltes, A. S. Tychkov, W. Hogervorst, and W. Vassen, Phys. Rev. Lett. **97**, 080404 (2006).
[9] J. D. Weinstein, R. deCarvalho, T. Guillet, B. Friedrich, and J. M. Doyle, Nature (London) **395**, 148 (1998).
[10] R. J. W. Stas, J. M. McNamara, W. Hogervorst, and W. Vassen, Phys. Rev. A **73**, 032713 (2006).

[11] S. J. M. Kuppens, J. G. C. Tempelaars, V. P. Mogendorff, B. J. Claessens, H. C. W. Beijerinck, and E. J. D. Vredenbregt, Phys. Rev. A **65**, 023410 (2002).
[12] A. S. Tychkov, T. Jeltes, J. M. McNamara, P. J. J. Tol, N. Herschbach, W. Hogervorst, and W. Vassen, Phys. Rev. A **73**, 031603 (2006).
[13] P. Spoden, M. Zinner, N. Herschbach, W. J. van Drunen, W. Ertmer, and G. Birkl, Phys. Rev. Lett. **94**, 223201 (2005).
[14] H. C. Busch, M. K. Shaffer, E. M. Ahmed, and C. I. Sukenik, Phys. Rev. A **73**, 023406 (2006).
[15] H. Katori and F. Shimizu, Phys. Rev. Lett. **73**, 2555 (1994).
[16] M. Walhout, U. Sterr, C. Orzel, M. Hoogerland, and S. L. Rolston, Phys. Rev. Lett. **74**, 506 (1995).
[17] W. Vassen, C. Cohen-Tannoudji, M. Leduc, D. Boiron, C. I. Westbrook, A. Truscott, K. Baldwin, G. Birkl, P. Cancio, and M. Trippenbach, Rev. Mod. Phys. **84**, 175 (2012).
[18] S. K. Lee, H. S. Lee, J. M. Kim, and D. Cho, J. Phys. B **38**, 1381 (2005).
[19] A. Mosk, S. Jochim, H. Moritz, T. Elsässer, M. Weidemüller, and R. Grimm, Opt. Lett. **26**, 1837 (2001).
[20] L. S. Cruz, M. Sereno, and F. C. Cruz, Opt. Express **16**, 2909 (2008).
[21] M. Eichhorn, M. Mudrich, and M. Weidemüller, Opt. Lett. **29**, 1147 (2004).
[22] P. Blythe, B. Roth, U. Fröhlich, H. Wenz, and S. Schiller, Phys. Rev. Lett. **95**, 183002 (2005).
[23] V. Vuletić, C. Chin, A. J. Kerman, and S. Chu, Phys. Rev. Lett. **81**, 5768 (1998).
[24] N. Poli, R. J. Brecha, G. Roati, and G. Modugno, Phys. Rev. A **65**, 021401 (2002).
[25] H. Katori and F. Shimizu, Jpn. J. Appl. Phys. **29**, L2124 (1990).
[26] P. D. Edmunds and P. F. Barker, Rev. Sci. Instrum. **84**, 083101 (2013).
[27] J. Grucker, J. Baudon, F. Perales, G. Dutier, G. Vassilev, V. Bocvarski, and M. Ducloy, J. Phys. B **41**, 021001 (2008).
[28] M. Batz, P.-J. Nacher, and G. Tastevin, J. Phys. Conf. Ser. **294**, 012002 (2011).
[29] J. Robert, V. Bocvarski, I. Colomb de Daunant, G. Vassilev, and J. Baudon, J. Phys. USSR **45**, 225 (1984).
[30] S. Kasai, R. Mizutani, R. Kondo, M. Hasuo, and T. Fujimoto, J. Phys. Soc. Jpn. **72**, 1936 (2003).
[31] J. Kolts and D. Setser, J. Chem. Phys. **68**, 4848 (1978).
[32] K. Tachibana, Phys. Rev. A **34**, 1007 (1986).
[33] A. Bogaerts and R. Gijbels, Phys. Rev. A **52**, 3743 (1995).
[34] A. Mosk, S. Kraft, M. Mudrich, K. Singer, W. Wohlleben, R. Grimm, and M. Weidemüller, Appl. Phys. B **73**, 791 (2001).
[35] R. Jáuregui, N. Poli, G. Roati, and G. Modugno, Phys. Rev. A **64**, 033403 (2001).
[36] R. W. Molof, H. L. Schwartz, T. M. Miller, and B. Bederson, Phys. Rev. A **10**, 1131 (1974).
[37] J. Mitroy, M. Safronova, and C. W. Clark, J. Phys. B **43**, 202001 (2010).